



Enhancing Sodium Ion Transport in a PEO-Based Solid Polymer Electrolyte System with NaAlO₂ Active Fillers

Arvind Kumar Chauhan^{1,4} · Kuldeep Mishra² · Deepak Kumar³ · Amarjeet Singh⁴

Received: 5 April 2021 / Accepted: 8 June 2021 / Published online: 16 June 2021
© The Minerals, Metals & Materials Society 2021

Abstract

This work reports the effect of sodium aluminate (NaAlO₂) filler particles on the ion dynamics of a solid polymer electrolyte system comprising polyethylene oxide, sodium perchlorate (NaClO₄) and propylene carbonate. Free-standing flexible polymer electrolyte films were obtained by solution-casting technique. The effect of NaAlO₂ fillers in the Na⁺ transport in the electrolyte system has been investigated using various physical and electrochemical studies. Scanning electron microscopy and X-ray diffraction studies reveal the enhanced amorphicity of the polymer electrolyte system upon dispersion of NaAlO₂ fillers. The undispersed polymer electrolyte displays a maximum ionic conductivity of $1.6 \times 10^{-5} \text{ S cm}^{-1}$ at 25°C, which increases to $7.4 \times 10^{-5} \text{ S cm}^{-1}$ on dispersion of 5 wt.% NaAlO₂ fillers at 30°C. The ion mobility and enhanced free ion numbers in the dispersed polymer electrolyte system are well-observed in the frequency-dependent dielectric studies. The optimized composition shows a significantly improved Na⁺ transport number of ~ 0.60 and electrochemical stability window of ~ 4.5 V.

Keywords NaAlO₂ filler · polymer electrolyte · sodium ion conductor · ion dynamics · Na⁺ transport number

Introduction

In last few years sodium-based energy storage devices such as sodium ion batteries (SIBs), room temperature sodium-sulfur (RT Na-S) batteries and sodium-ion capacitors (SICs), have been largely investigated and proposed as alternative to lithium-based systems.^{1–5} Electrolyte is an important component for any such device, which control the ion dynamics between the electrodes and hence the overall performance of the electrochemical system. Polymer-based electrolytes have gained tremendous attention in last few decades for their applications in energy storage devices.^{5,6} Due to a solid but

flexible polymer backbone, these electrolytes offer a wider working temperature range and scope of flexible device fabrication. Additionally, these electrolytes have potential to overcome the issues of conventionally used liquid electrolytes such as leakage and short-circuiting. Polyethylene oxide (PEO) is the oldest polymer and has been extensively studied for electrolyte preparation. In PEO-based electrolytes, due to presence of ether oxygen in its main chain, the cation transport occurs via hopping from one ether oxygen site to other. The ion hopping mechanism is more prominent when the polymer matrix is amorphous. In the case of PEO, its semi-crystallinity offers significant hindrance to the ionic motion, and hence, conventional salt-in-PEO systems, in general, display lower ionic conductivity ($< 10^{-6} \text{ S cm}^{-1}$) and are of limited use at room temperature.

In order to improve the ionic conductivity and other electrochemical properties of PEO-based electrolyte systems, two prominent approaches have been proposed: the first is plasticization, and the second is the dispersion of nano-/micro-size ceramic fillers. In plasticization, various organic carbonates, such as ethylene carbonate (EC), propylene carbonate (PC) and diethyl carbonate (DEC), low-molecular-weight polymers like polyethylene glycol (PEG), and various ionic liquids are immobilized in the polymer

✉ Kuldeep Mishra
mishkuldeep@gmail.com

¹ Department of Physics, Swami Premanand Mahavidyalaya, Mukerian, Hoshiarpur 144211, India

² Department of Physics and Materials Science, Jaypee University, Anoopshahr, Bulandshahr 203390, India

³ Electronics and Mechanical Engineering School, Affiliated to Gujarat Technological University, Vadodara, Gujarat 390008, India

⁴ Department of Physics, Himachal Pradesh University, Summer Hill, Shimla 171005, India

matrix. These liquid plasticizers enhance amorphicity in the polymer matrix and support the ion dissociation as well. On the other hand, the dispersion of nano-/micro-sized metal oxide particles, such as SiO₂, Al₂O₃, TiO₂, BaTiO₃, ZnFe₂O₄, etc., enhance the entropy of the system by creating disturbance in the crystalline orientation of the polymers and hence, promote the ion transport through the faster segmental motion.^{7–13} Additionally, the filler particles with acidic nature hold the anions on their surface via hydrogen bonding and set more cations free in the electrolyte system.¹³ The greater contribution of the cations in the total conductivity of the electrolyte system is much required for rechargeable battery systems. A few functionalized carbon structures have also been investigated as fillers in PEO-based electrolytes. Ma et al.¹⁴ used carbon quantum dots (CQDs) enriched with oxygen-containing functional groups in a PEO/CQDs-Na electrolyte system. The Lewis acid–base interactions between CQD and salt enabled easy Na ion transport, which is reflected well in terms of the enhanced ionic conductivity and Na⁺ transport number. Sulfonated graphene oxide (sGO) filler has been reported to produce single-ion (Li⁺) conducting electrolyte in lithiated Nafion nanocomposite.¹⁵

The ion conduction in the all the above composite electrolytes is based upon the Lewis acid–base interaction between the salt and polymer, and the enhanced amorphicity of the polymer network. In the last few years, a new type of ceramic filler has been proposed which has a specific cation in its main chemical structure. These fillers are called active fillers, as they directly participate in the ion conduction by providing extra cations and pushing cationic motion in the electrolytes. Zhang et al.¹⁶ demonstrated three-fold enhancement in the ionic conductivity and superior thermal and electrochemical stability in an active NASICON structured Na_{3.4}Zr_{1.8}Mg_{0.2}Si₂PO₁₂ ceramic filler dispersed PEO-sodium bis(trifluorosulfonyl)imide (NaTFSI) electrolyte system. Recently, Wang et al.¹⁷ reported a composite polymer electrolyte of PEO plus sodium bis(trifluoromethylsulfonyl)imide (NaTFSI) dispersed with a NASICON-type Na₃Zr₂Si₂PO₁₂ (NZSP) nanostructured framework. They obtained superior ionic conductivity (1.4 × 10⁻⁴ S cm⁻¹) and mechanical strength when filler particles were introduced. NASICON-type active fillers have also been studied in liquid-rich (gel) polymer electrolyte systems. Sodium aluminate (NaAlO₂) has also been investigated as active filler in polymer electrolyte systems. Hashmi et al.¹⁸ reported a significant jump in the Na⁺ transport number, from 0.27 to 0.42, on dispersion of NaAlO₂ fillers in a gel polymer electrolyte system as compared to passive Al₂O₃ fillers. They also observed enhancement in ionic conductivity and electrochemical stability. In an earlier study, we demonstrated active role of NaAlO₂ fillers in enhancing electrochemical properties of poly(vinylidene fluoride-cohexafluoropropylene) (PVdF-HFP)-based porous gel polymer

electrolyte.¹⁹ The abovementioned NaAlO₂ dispersed polymer electrolytes^{18,19} are gel in nature wherein the ionic conduction mechanism is different than the PEO-based solid polymer electrolytes. It will be interesting to see the effect of these NaAlO₂ fillers on the structural and electrochemical properties of PEO-based sodium-ion-conducting solid polymer electrolytes.

In the present work, an attempt is made to enhance the electrochemical properties of a polymer electrolyte system comprising PEO, NaClO₄ and PC by dispersing NaAlO₂ fillers. The effect of fillers on structural and electrochemical properties of the electrolyte system has been investigated by using X-ray diffraction (XRD), scanning electron microscopy (SEM), complex impedance spectroscopy, cyclic voltammetry (CV) and linear sweep voltammetry. Various frequency-dependent parameters obtained from the impedance spectroscopy such as real and imaginary parts of dielectric constant, loss tangent and AC conductivity are investigated to explore the ion dynamics in the prepared electrolyte system. An ion transport model in three different phases of NaAlO₂ dispersed solid polymer electrolytes is also presented in this paper.

Experimental

Materials

The precursors, poly(ethylene oxide) (PEO, M_w ~ 1 × 10⁵), sodium perchlorate (NaClO₄, purity ≥ 98%), propylene carbonate (PC, purity ≥ 99.7%) and sodium aluminate (NaAlO₂, purity ≥ 99.95%) powder were purchased from Aldrich. The solvent acetonitrile (99.5 %) was procured from SRL, India.

Preparation of NaAlO₂ Dispersed Solid Polymer Electrolyte Films

The polymer electrolyte films carrying different concentrations of NaAlO₂ filler were prepared by solution-casting technique. Initially, the stoichiometric amounts of polymer PEO and NaClO₄ salt (9:1 wt./wt.) were dissolved in acetonitrile solvent with continuous stirring for 10 h at room temperature. The plasticizer PC (10 wt.% of PEO) was added to the above solution during the stirring. The NaAlO₂ powder was dispersed in varying amounts according to the compositional formula PEO + *x* NaAlO₂, where *x* = 0, 2, 5, 7, 8.5 and 10 wt.%. After addition of NaAlO₂ powder, various solutions of PEO/NaClO₄/PC/NaAlO₂ were subjected to continuous stirring for 24 h to ensure homogeneous dispersion of the NaAlO₂ particles. The obtained homogeneous solutions were poured into a petri dish and left for slow solvent evaporation at ambient conditions. After evaporation of the solvent, free-standing and flexible polymer films

were obtained (Fig. 1). The films with more than 10 wt.% NaAlO₂, were not stable, and phase separation was observed.

Characterization

The structural and morphological studies of the polymer electrolyte system were carried out by X-ray diffraction (XRD-6000, SHIMADZU) and scanning electron microscopy (SEM, Zeiss EVO-MA15) techniques. The crystallinity of the polymer electrolyte films was measured using the respective XRD pattern, using the formula:

$$\chi_c = \frac{A}{A_o} \times 100\% \quad (1)$$

where A = area under crystalline peaks, and A_o = total area under the diffractogram (crystalline plus amorphous).

All the electrical and electrochemical measurements such as impedance spectroscopy, linear sweep voltammetry (LSV), and polarization measurements were performed using an electrochemical analyzer (Zive SP1) of WonATech Co., Ltd., Korea. For the ionic conductivity measurement, the films were sandwiched between two stainless-steel (SS) ion-blocking electrodes of area 1 cm², and an alternating voltage of 10 mV was applied across the cell SS|polymer electrolyte|SS over the frequency (f) range 1 Hz–1 MHz. The obtained real (Z') and imaginary (Z'') part of the impedance data were used to evaluate various frequency-dependent parameters including the real (ϵ') and imaginary (ϵ'') part of the dielectric constant, loss tangent ($\tan \delta$) and AC conductivity (σ_{ac}).

To obtain the ion transference number (t_{ion}), DC polarization technique was used on the cell configuration: SS|polymer electrolyte|SS. A DC potential of 0.5 V was applied to the above cell, and the current was recorded with respect to time. The total ion transport number (t_{ion}) was evaluated using the following formula:

$$t_{ion} = \left(1 - \frac{i_s}{i_T} \right) \quad (2)$$

where i_T and i_s are total (ion + electron) and residual currents, respectively.

The Na⁺ transport number (t_{Na^+}) in the polymer electrolyte system was calculated using a combination of AC and DC techniques suggested by Vincent and his co-workers.^{20,21} A DC polarization experiment was performed on the symmetrical cell with a reversible Na-Hg electrode as Na-Hg|polymer electrolyte|Na-Hg. As part of the technique, impedance data of the above cell was taken before and after the polarization. The Na⁺ transport number (t_{Na^+}) was obtained using the formula:

$$t_{Na^+} = \frac{I_s}{I_o} \cdot \left(\frac{\Delta V - R_o I_o}{\Delta V - R_s I_s} \right) \quad (3)$$

where I_s is saturation current, I_o is the initial current, ΔV is the applied small DC voltage (16 mV) in the polarization, R_o is impedance before polarization and R_s is impedance after polarization.

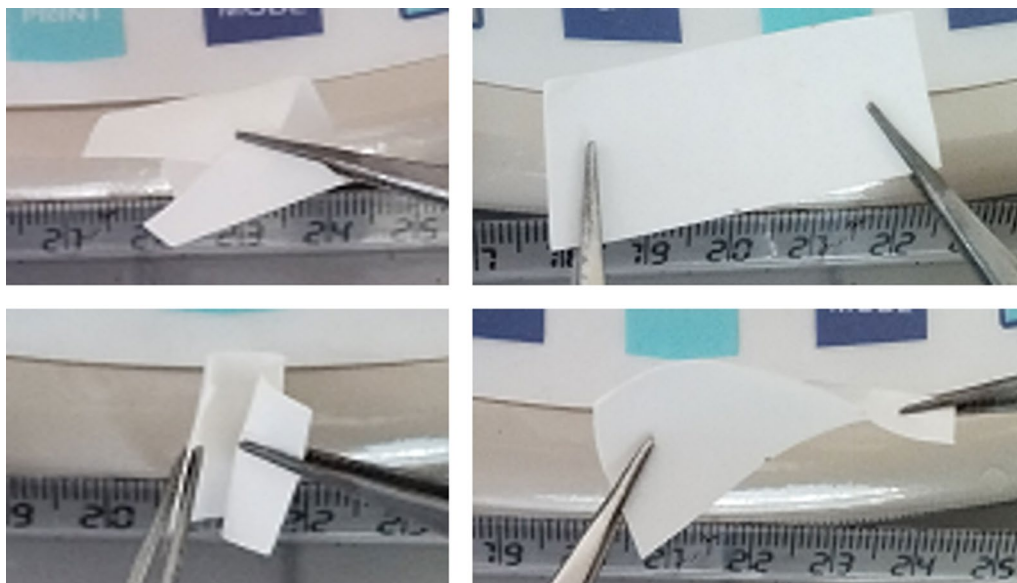


Fig. 1 Photograph of the typical polymer electrolyte film in different bending modes.

Results and discussion

XRD studies

To examine the influence of NaAlO₂ as filler particles on the crystalline structure of PEO-NaClO₄-PC, X-ray diffraction (XRD) patterns were recorded and are shown in Fig. 2. The two most distinctive characteristic peaks, a single peak at 19.1° and a triple peak at about 23.3°, are in good agreement with the results obtained by other authors for pure PEO polymer film.^{10,12,17,22–24} The crystallinity of pure PEO was obtained as 76%. The intensity of the characteristic crystalline peaks of PEO reduced significantly when NaClO₄ and PC were immobilized in the PEO matrix to obtain the solid polymer electrolyte. The degree of crystallinity, obtained using Eq. 1, for the undispersed PEO-NaClO₄-PC solid polymer electrolyte was determined to be 31%. However, on dispersing the 5 wt.% NaAlO₂ particles in PEO-NaClO₄-PC matrix, the characteristic single peak at 19.1° decreased drastically, and the degree of crystallinity dropped to 26%. For the 10 wt.% composition, although the peak at 19.1° increased in height, the other peak at 23.3° reduced significantly, and the overall crystallinity of this polymer electrolyte membrane reduced to 25%. Thus, on incorporating the NaClO₄ and PC, the crystallinity of the PEO was significantly reduced. The crystallinity was further suppressed on dispersion of NaAlO₂ particles within the PEO framework. The higher amorphicity thus

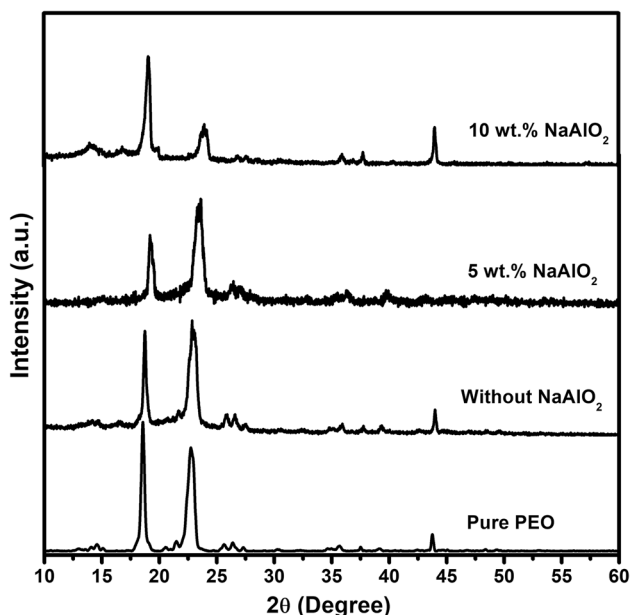


Fig. 2 X-ray diffractograms of pure PEO and different compositions of the NaAlO₂ dispersed polymer electrolyte system.

obtained provided a flexible electrolyte backbone which supports better ion transport through it.

Scanning electron microscopy (SEM) studies

The SEM images of polymer electrolytes with 5 wt.%, 10 wt.% NaAlO₂ and without NaAlO₂ are shown in Fig. 3. Figure 3a shows the micrograph of the undispersed PEO-NaClO₄-PC polymer electrolyte. The spherical semicrystalline regions, referred to as spherulites, enclosed with a fibrous texture are observed throughout the surface of the solid polymer electrolyte film. However, with the dispersion of NaAlO₂ particles in PEO-NaClO₄-PC, significant morphological changes are observed. Figure 3b shows the micrograph of the optimized electrolyte composition dispersed with 5 wt.% NaAlO₂ content. The NaAlO₂ particles seem to fill up the granular regions of PEO-NaClO₄-PC matrix, thereby resulting in a uniform flat surface morphology. However, for 10 wt.% NaAlO₂ dispersion (Fig. 3c), the electrolyte membrane presents an uneven surface morphology, and NaAlO₂ particles appear to be distributed over the entire surface. It is important to note that NaAlO₂ particles may efficiently wrap and absorb the NaClO₄-PC salt solution around them for a certain low concentration (5 wt.% NaAlO₂),^{17,25} thereby contributing to the coordinated ion-transport behavior within the optimized electrolyte system.

Ionic conductivity studies

The variation of ionic conductivity of the polymer electrolyte system with NaAlO₂ filler concentration is shown in Fig. 4a. The ionic conductivity initially increases with increase in NaAlO₂ concentration and jumps from $\sim 1.6 \times 10^{-5} \text{ S cm}^{-1}$ to $\sim 7.4 \times 10^{-5} \text{ S cm}^{-1}$ for the electrolyte composition with 5 wt.% NaAlO₂. After the above threshold concentration, the ionic conductivity decreases, and the observed minimum is $\sim 8.9 \times 10^{-6} \text{ S cm}^{-1}$ for the composition with 10 wt.% NaAlO₂. The initial increase in the conductivity is associated with the enhanced amorphicity of the electrolyte system, which promotes the faster ion transport through the disordered polymer chains. Additionally, the presence of NaAlO₂ fillers in their polar form of Na⁺-AlO₂⁻ not only set more Na⁺ ions free but can also provide easy pathway for Na⁺ transport.^{18,19} The drop in the ionic conductivity after 5 wt.% NaAlO₂ may be associated with the blocking nature of the polar NaAlO₂ fillers. At higher concentration, NaAlO₂ fillers block the Na⁺ transport and hence reduce the ion mobility. The higher fluctuation in the ionic conductivity of the composition with 8.5 and 10 wt.% NaAlO₂ is associated with the presence of nonhomogeneous dispersion of the filler particles in the polymer matrix at such higher concentrations.

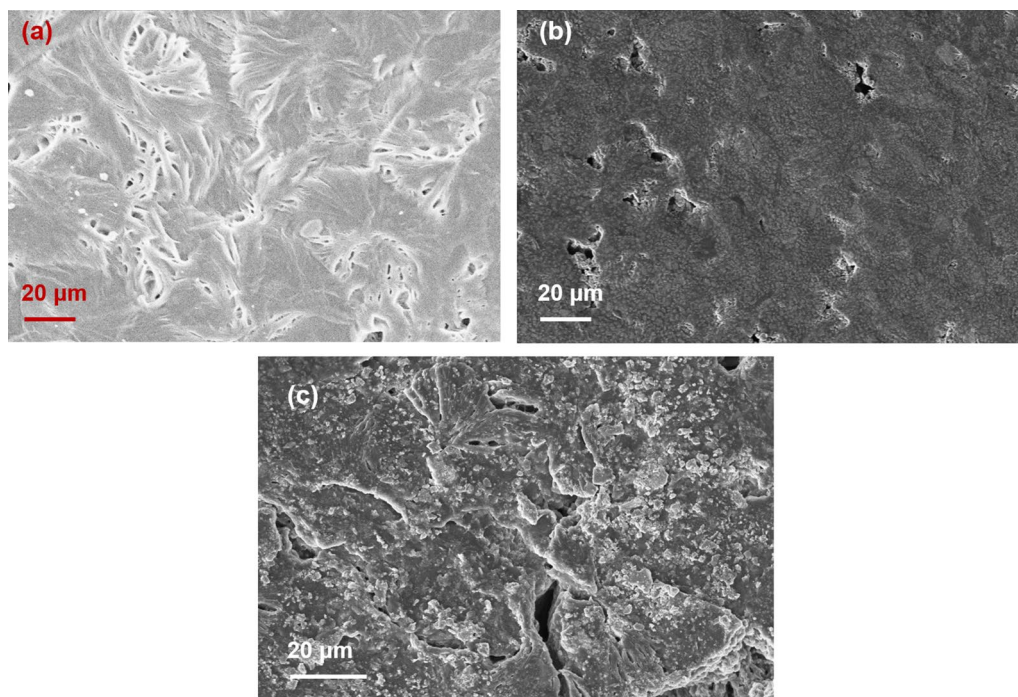


Fig. 3. SEM image of polymer electrolyte (a) without NaAlO_2 , (b) with 5 wt.% NaAlO_2 and (c) with 10 wt.% NaAlO_2 .

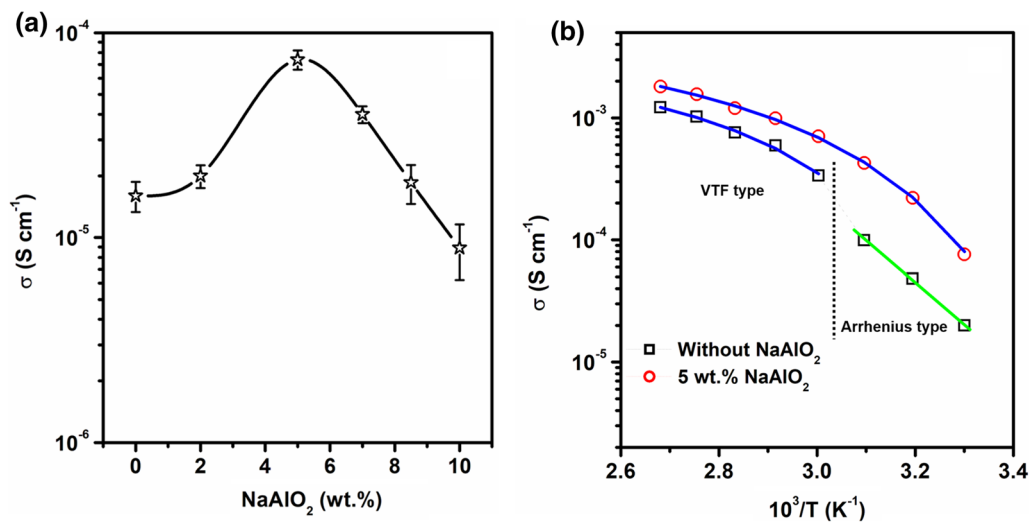


Fig. 4 (a) Variation of ionic conductivity with NaAlO_2 concentration in polymer electrolyte at room temperature (30°C) and (b) temperature-dependent ionic conductivity of polymer electrolyte without

NaAlO_2 and with 5 wt.% NaAlO_2 . (Blue lines are VTF fitted, and the green line is Arrhenius fitted).

The temperature dependence of the ionic conductivity patterns of undispersed polymer electrolyte and the highest conducting composition with 5 wt.% NaAlO_2 films are shown in Fig. 4b. The composition without filler shows two different behaviors in its pattern, separated by a dotted line in Fig. 4b. In the temperature ranging from

30°C to 50°C , the electrolyte follows Arrhenius behavior, which is typical of semicrystalline polymer electrolyte. In this phase, the enhancement in the conductivity is more thermally activated than the contribution of the molecular motion of polymer host.²⁶ The Arrhenius equation of the ion-transport behavior is given as:

$$\sigma = \sigma_0 \exp\left(\frac{-E_a}{K_B T}\right) \tag{4}$$

where σ_0 , E_a and K_B are the pre-exponential factor, activation energy and Boltzmann constant, respectively. The obtained value of the activation energy, using the Arrhenius fitting, for the undispersed polymer electrolyte in the above-mentioned temperature range is obtained as 0.29 eV, which is quite low and sufficient for polymer electrolytes. The sudden increase in the conductivity between 50°C and 60°C is associated with the melting of the crystalline phase of PEO to an amorphous phase. This type of transition is typically observed in PEO-based solid polymer electrolytes.²⁶ Above 60°C, the polymer becomes amorphous, and the system retains free volumes. This endorses segmental motion in the polymer electrolyte and hence promotes the ion mobility. In this temperature range, the conductivity of undispersed composition follows the Vogel–Tammann–Fulcher (VTF) model of ion transport. The VTF equation is given as:

$$\sigma = AT^{-1/2} \exp\left[\frac{-B}{K_B(T - T_0)}\right] \tag{5}$$

where A is the pre-exponential factor related to the number of ions, K_B is the Boltzmann constant, B is the pseudo-activation energy associated with the polymer segmental motion and T_0 is the temperature close to glass transition temperature and corresponds zero configurational entropy. The values of the VTF parameters are given in Table I for both the electrolyte compositions along with the regression (R^2) values close to unity. In the case of 5 wt.% NaAlO₂, the conductivity is found to follow the VTF behavior in the complete temperature range of measurement, i.e., 30–100°C. This is due to the dominating role of polymer segmental motion in the ion transport which is well assisted with the enhanced amorphicity in the polymer electrolyte on dispersion of NaAlO₂ fillers. This is well corroborated with the findings of XRD and SEM studies. The conductivity of the dispersed polymer electrolyte remains superior to the undispersed one throughout the temperature range. Additionally, the value of pre-exponential factor A , which is related to free ions, is found greater in the case of composition with 5 wt.% NaAlO₂. This is an indication that the NaAlO₂ filler enhances free ion concentration in the polymer electrolytes.

Table I VTF fitting parameters for the polymer electrolyte without and with 5 wt.% NaAlO₂.

Composition	A (S cm ⁻¹ K ^{1/2})	B (eV)	T_0 (K)	R^2
Without NaAlO ₂ *	0.09	0.012	293.61	0.9964
5 wt.% NaAlO ₂	0.19	0.016	265.55	0.9987

*In the temperature range 60–100°C

The value of T_0 is also decreased in the NaAlO₂ dispersed composition, which indicates the possible decrease in the glass transition temperature of the polymer electrolyte system.

Frequency-dependent dielectric constant (ϵ' and ϵ''), AC conductivity (σ_{ac}) and loss tangent ($\tan \delta$) studies

In order to understand the role of NaAlO₂ fillers in the ion dynamics of the solid polymer electrolyte system, frequency-dependent parameters ϵ' , ϵ'' , σ_{ac} and $\tan \delta$ are investigated. The number of charge carriers (n) has strong dependency on the dielectric constant (ϵ), as;

$$n = n_0 \exp\left(\frac{-U}{\epsilon K_B T}\right) \tag{6}$$

The frequency-dependent dielectric constants, i.e., real (ϵ') and imaginary (ϵ''), are shown in Fig. 5a and b for all the compositions of the polymer electrolyte system. The higher values of ϵ' and ϵ'' at low frequencies are due to the space charge effect associated with the accumulated charges at the ion-blocking electrode leading to high polarization and hence high dielectric constant. The above space charge accumulation is found increasing up to 5 wt.% NaAlO₂, and after that a drop is observed for the composition with 7 wt.% NaAlO₂. In the case of 8.5 and 10 wt.% NaAlO₂, a jump is observed in the ϵ' and ϵ'' values at 1 Hz. The increase in ϵ' and ϵ'' values is attributed to the dipolar mismatches due to the enhanced localized charge carriers at the charge defect centers. At the higher frequencies, the charged dipoles fail to respond to the field values and high frequency relaxation process corresponding to the segmental motion of the polymer chains dominating.^{12,27–29} This results in a decrease in the dielectric constant of the electrolyte material. Interestingly, the composition with 8.5 and 10 wt.% NaAlO₂ display a different behavior in the ϵ' plot. The values of ϵ' for the above compositions are found slightly higher than the highest conducting composition, i.e., polymer electrolyte with 5 wt.% NaAlO₂, in the high-frequency range. This may be due to the significantly high numbers of free charge carriers in the electrolyte film as an effect of higher filler concentration. At higher frequencies, where the dielectric loss occurs due to the de-acceleration and acceleration of ions through the segmental motion, the values of ϵ'' (Fig. 5b) remain lower for the compositions with 8.5 and 10 wt.% NaAlO₂. This indicates that these compositions carry significant numbers of charge carriers, but the ion mobility is hindered.

In order to understand the effect of NaAlO₂ filler on the segmental relaxation in the electrolyte system, the variation of the loss tangent ($\tan \delta = \frac{\epsilon''}{\epsilon'}$) for various compositions of the electrolyte system is shown in Fig. 5c. The

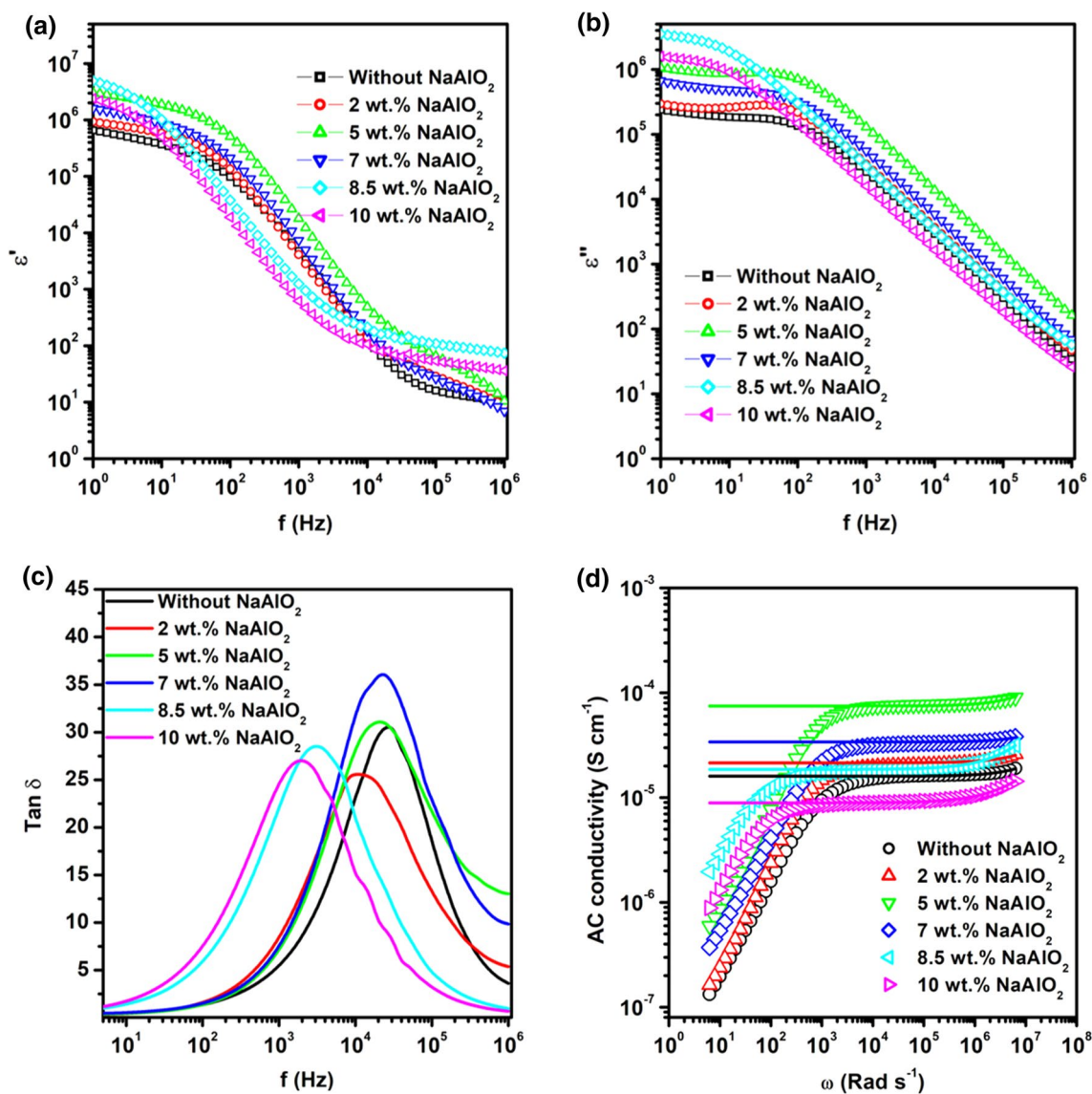


Fig. 5 Frequency dependence of (a) real part ϵ' and (b) imaginary part (ϵ'') of the dielectric constant, (c) loss tangent and (d) AC conductivity for the various compositions of the NaAlO_2 dispersed polymer electrolyte system.

presence of the peak in the figure is due to the maximum energy transfer at the particular frequency, and it is associated with the ion transfer through the segmental motion of the polymer matrix in the electrolyte system. It is observed that the position of the peaks slightly shifted towards the lower-frequency side on dispersion of NaAlO_2 fillers, and this shift becomes significant for the composition with 10 wt.% NaAlO_2 . The position of this relaxation peak provides the relaxation time (τ), as $\tau = 1/2\pi f$, where f is the frequency at the peak. The obtained values of the relaxation time for various compositions of the polymer electrolyte systems are listed in Table II. It is observed that the relaxation time is increased on dispersion of the fillers, and

Table II Relaxation time (τ) and the parameters obtained from the JPL fitting.

Composition	τ (μs)	JPL parameters		
		σ_{dc} (S cm^{-1})	A	η
Without NaAlO_2	6.14	1.60×10^{-5}	1.14×10^{-12}	0.92
2 wt.% NaAlO_2	14.44	2.15×10^{-5}	8.05×10^{-12}	0.87
5 wt.% NaAlO_2	7.9	7.50×10^{-5}	1.12×10^{-11}	0.90
7 wt.% NaAlO_2	7.13	3.41×10^{-5}	2.32×10^{-12}	0.93
8.5 wt.% NaAlO_2	39.8	1.80×10^{-5}	4.66×10^{-11}	0.80
10 wt.% NaAlO_2	83.41	8.92×10^{-6}	4.50×10^{-11}	0.76

it is maximum for the composition with 10 wt.% NaAlO₂. In general, this peak is shifted towards higher frequencies on addition of fillers,^{29,30} which is associated with the lesser relaxation time or faster segmental motion. The relaxation time for the highest conducting composition, i.e., composition with 5 wt.% NaAlO₂, appears close to that of the undispersed composition. The opposite behavior in the case of NaAlO₂ active fillers may be associated with the blocking nature of these particles at higher concentration. At higher concentration of NaAlO₂, though the amorphicity of the polymer matrix has been increased, the fillers entangled in the matrix do not allow faster segmental motion for the ion transport.

In order to further investigate the ion transport, the AC conductivity pattern of the electrolyte composition is shown in Fig. 5d. The conductivity pattern is found to follow Jonscher’s power law (JPL)³¹ given as:

$$\sigma = \sigma_o + A\omega^\eta \tag{7}$$

where σ_o is the DC conductivity, A is the pre-exponential factor and η is the fractional exponent which explains the type of motion of the ions through the matrix. The value of η may be 0, $0 < \eta < 1$ or > 1 , depending on free hopping, correlated hopping and caged ion motion, respectively.^{32–34} The solid lines in Fig. 5d are JPL fitted lines, and the obtained parameters are listed in Table II. The deviation of the obtained conductivity pattern for the JPL lines in the low-frequency range is associated with the electrode polarization effect. The plateau region of the pattern provides the DC conductivity (σ_{dc}) of the respective electrolyte composition. The value of the exponent η is obtained below unity for all the compositions and is minimum for 10 wt.% NaAlO₂. This indicates that the ionic motion in the electrolyte system is a correlated one. The η is considered as the ratio of backward ion hopping to the site relaxation time.³⁴ Values of the exponent less than unity reveal the dominance of backward hopping of ions when the NaAlO₂ fillers are introduced in greater amount.

The quantitative assessment of the ion dynamics in the active NaAlO₂ filler dispersed polymer electrolyte system is done with the help of parameters such as DC conductivity (σ_{dc}), maximum tangent loss ($\tan \delta_{max}$) and corresponding frequency (f_{max}), obtained from the frequency-dependent dielectric analysis. The free ion number density (N) and the ion mobility (μ) in this electrolyte system are obtained using the following relations:^{35,36}

$$N = \frac{\sigma_{dc} K_B T}{Dq^2} \tag{8a}$$

$$\mu = \frac{\sigma_{dc}}{qN} \tag{8b}$$

where D is the diffusivity ($D = \frac{2\pi f_{max} d^2}{32(\tan \delta_{max})^3}$), d is the thickness of the electrolyte film and q is the elementary charge.

The variation of N and μ with concretion of NaAlO₂ fillers in the polymer electrolyte system is shown in Fig. 6. The ion mobilities of the compositions with 2 and 5 wt.% NaAlO₂ are obtained as 4.62×10^{-3} and 5.30×10^{-3} cm² V⁻¹ s⁻¹, respectively, which are slightly lower but close to that of the undispersed composition, i.e., 5.33×10^{-3} cm² V⁻¹ s⁻¹. At higher filler concentrations, the mobility drops significantly. This is attributed to the ion-blocking nature of the active polar filler. The free ion number density (N) rapidly increased in the NaAlO₂ dispersion, and the found maximum was $\sim 8.67 \times 10^{16}$ cm⁻³ for the highest-conducting composition carrying 5 wt.% NaAlO₂. The compositions with 7, 8.5 and 10 wt.% NaAlO₂ carry close N values of $\sim 6.42 \times 10^{16}$, 8.60×10^{16} and 6.27×10^{16} cm⁻³, respectively. These N values are more than threefold as compared to the undispersed composition. These observations reveal that the initial increase in the ionic conductivity is associated with the dominance of free charge carriers, and after 5 wt.% NaAlO₂, the reduction in the ion mobility causes a conductivity dip.

From the above discussion, it is clear that the NaAlO₂ fillers help in the ion dissociation and provide extra Na ions in the solid polymer electrolyte system. However, their excess amount in the polymer matrix hinders the ionic motion. The ion transport in the PEO-NaClO₄-PC-NaAlO₂ polymer electrolyte system in demonstrated in Fig. 7. In the undispersed polymer electrolyte composition, the Na⁺ transport take place through the hopping mechanism from one ether oxygen to other. The plasticizer PC provides good amorphicity

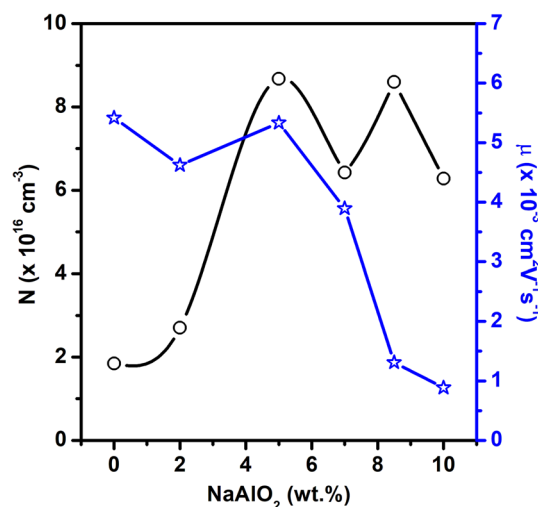


Fig. 6 Variation of free ion number density (N) and mobility (μ) with NaAlO₂ concentration in polymer electrolyte at room temperature (30°C).

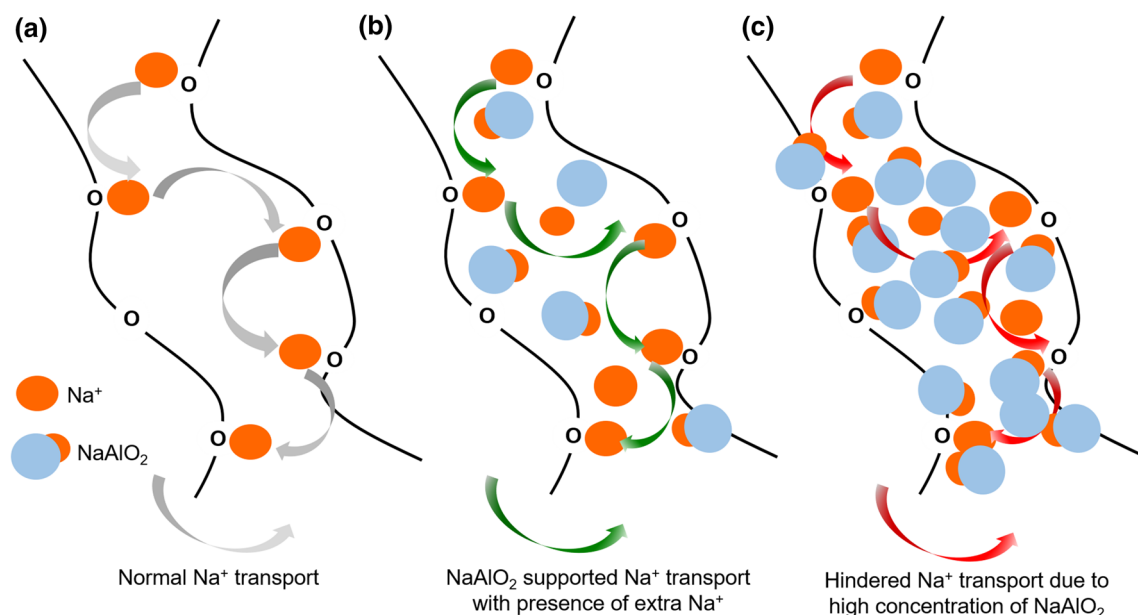


Fig. 7 Ion conduction model demonstrating the Na^+ ion transport in three different phases of the NaAlO_2 dispersed polymer electrolyte system.

to the polymer matrix which results in fast Na^+ transport through segmental motion of the polymer matrix (Fig. 7a). On dispersion of the optimum amount of NaAlO_2 fillers, the number of Na ions is enhanced significantly, and ion mobility is supported by the active NaAlO_2 fillers (Fig. 7b). However, on dispersion of higher content of NaAlO_2 filler, the free ion number density is affected by the polar $\text{Na}^+\text{-AlO}_2^-$ due to the formation of an ion multiplate, and additionally, cation transport is hindered as the filler particles block them by occupying their path and ether oxygen sites (Fig. 7c).

Electrochemical stability window (ESW) and ion transport number

In order to see the effect of active NaAlO_2 fillers on the ESW of the polymer electrolyte system, linear sweep voltammetry (LSV) was performed on the electrolyte system. The LSV traces of the undispersed and the optimized NaAlO_2 dispersed (5 wt. %) polymer electrolyte films are shown in Fig. 8a. The ESW of the optimized composition is found superior (~ 4.5 V) than the undispersed one (~ 3.7 V). This feature is in accordance with the earlier reports on gel polymer electrolytes dispersed with NaAlO_2 fillers.^{18,19}

To confirm the purely ionic nature of the polymer electrolyte system, the ion transport number was measured using the DC polarization technique, as discussed in the “Characterization” section. Figure 8b shows the DC polarization curve for the optimized polymer electrolyte film (5 wt. % NaAlO_2). In the polarization curve of the cell with the SS ion-blocking electrode, the value of the initial current (I_T)

is observed as $13.36 \mu\text{A cm}^{-2}$, which suddenly drops and saturates at $\sim 0.01 \mu\text{A cm}^{-2}$ (I_s). The ion transport number (t_{ion}) obtained using Eq. 2 is observed close to unity. Similar observations were made for all the other compositions of the NaAlO_2 dispersed polymer electrolyte system. This reveals that the prepared electrolyte system is purely ionic in nature.

To calculate the Na^+ ion transport number (t_{Na^+}) in the polymer electrolyte system, a combined AC and DC technique was used, as discussed in the “Characterization” section. Figure 8c and d shows the complex impedance plots obtained for the electrolyte compositions with 5 and 10 wt. % NaAlO_2 , respectively, with their respective DC polarization curves in the inset. In the DC polarization curves (inset Fig. 8c and d), where the reversible Na-Hg electrodes were used, the currents do not follow the pattern as for SS electrodes in Fig. 8b and saturates at higher current values. This is associated with the Na^+ conductivity in the polymer electrolyte, which does not fade with the Na-Hg reversible electrode. For the highest conducting composition, i.e., composition with 5 wt. % NaAlO_2 , the initial current (I_o) and the saturation current (I_s) are observed as $\sim 14.37 \mu\text{A cm}^{-2}$ and $8.41 \mu\text{A cm}^{-2}$, respectively. The complex impedance plots before and after the polarization (Fig. 8c) give the values of the bulk resistance before (R_o) and after (R_s) polarization as $\sim 424 \Omega$ and $\sim 759 \Omega$, respectively. The Na^+ transport number (t_{Na^+}) obtained using Eq. 3 is found as ~ 0.60 for the highest conducting composition carrying 5 wt. % NaAlO_2 filler. For the composition with the highest (10 wt. % NaAlO_2) dispersion, the values of the polarization currents, I_o and I_s , are obtained as $4.21 \mu\text{A cm}^{-2}$ and $1.40 \mu\text{A cm}^{-2}$, respectively, and the bulk resistance values, R_o and R_s , are obtained as 1326Ω and 5602Ω , respectively (Fig. 8d). The

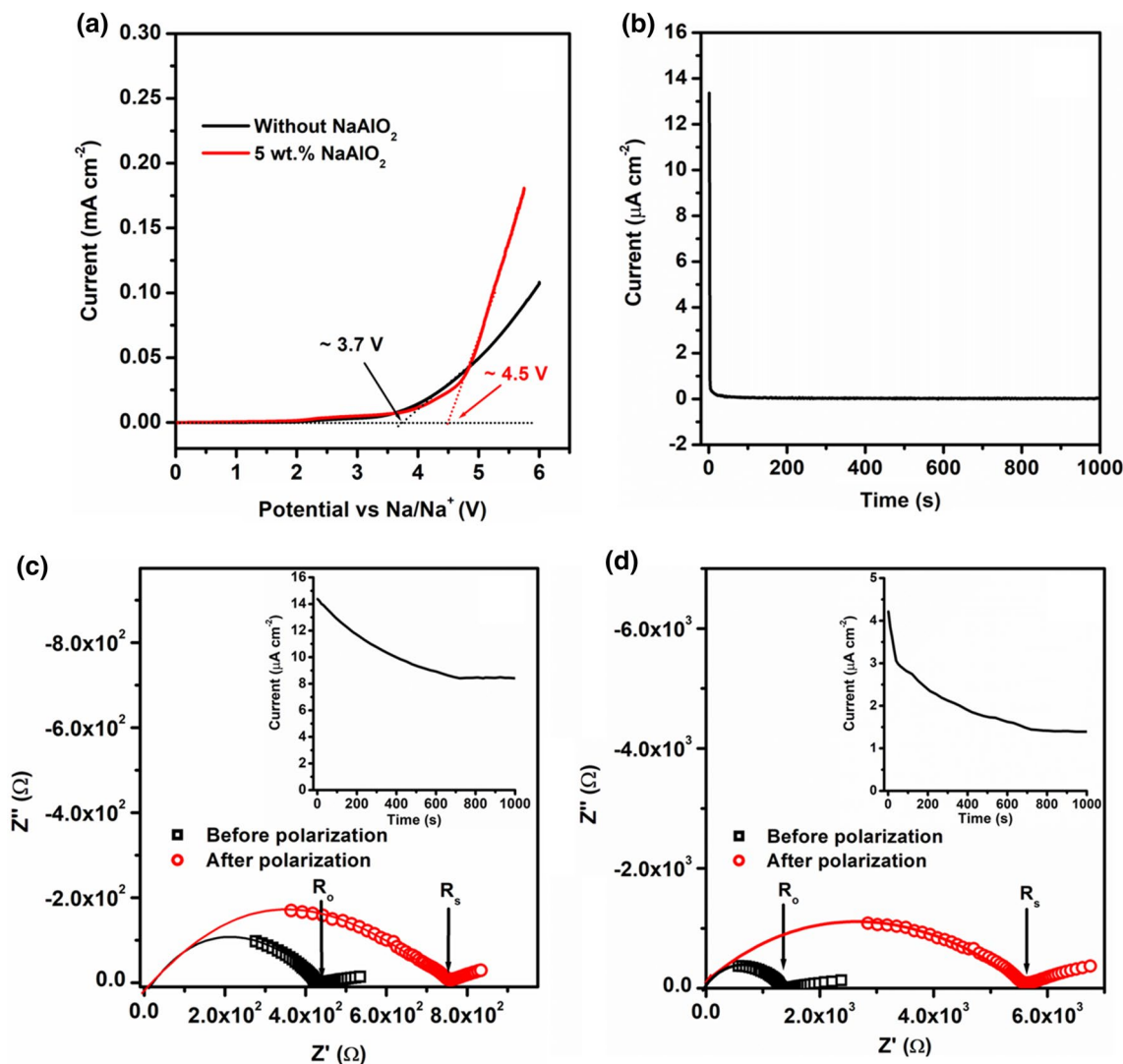


Fig. 8 (a) LSV traces of polymer electrolyte without NaAlO₂ and with 5 wt.% NaAlO₂, (b) DC polarization of polymer electrolyte film with 5 wt.% NaAlO₂ in symmetrical cell with blocking SS, (c) complex impedance plots and DC polarization curve (inset) of Na-

Hg|polymer electrolyte with 5 wt.% NaAlO₂ |Na-Hg cell and (d) complex impedance plots and DC polarization curve (inset) of Na-Hg|polymer electrolyte with 10 wt.% NaAlO₂ |Na-Hg cell reversible Na-Hg electrodes.

t_{Na^+} value for the above composition is evaluated to be ~ 0.42 . The t_{Na^+} value for the undispersed composition was obtained as ~ 0.32 . This reveals that the NaAlO₂ fillers enhance the contribution of Na⁺ transport in the total ionic conductivity of the electrolyte film; however, at higher filler concentration, the Na⁺ ion transport is hindered. These observations confirm the finding of the ion dynamics studies and support the ion transport model demonstrated in Fig. 7.

Conclusion

Free-standing and flexible polymer electrolyte films comprising PEO, NaClO₄ salt, PC plasticizer and varying concentrations of NaAlO₂ fillers were prepared. The effect of active NaAlO₂ fillers on the structural and electrical properties of a sodium-ion-conducting PEO-NaClO₄-PC

polymer electrolyte system was investigated. The following features were observed:

- (1) The NaAlO₂ fillers hinder the crystallization of the polymer and promote amorphicity in the polymer electrolyte. The crystallinity of the undispersed polymer electrolyte was observed as ~ 31%, which reduced to a minimum of ~ 25% for the composition with 10 wt.% NaAlO₂.
- (2) The ionic conductivity of the polymer electrolyte system ($\sim 1.6 \times 10^{-5} \text{ S cm}^{-1}$) increased with dispersion of fillers, with a maximum of $\sim 7.4 \times 10^{-5} \text{ S cm}^{-1}$ found for the composition with 5 wt.% NaAlO₂. The conductivity dropped on dispersion of higher content of NaAlO₂.
- (3) The enhanced amorphicity in the polymer electrolyte system was reflected well in the temperature-dependent conductivity pattern of the NaAlO₂ dispersed polymer electrolyte system, as it followed VTF behavior in the entire temperature range.
- (4) The ion dynamics in the electrolyte system were investigated using frequency-dependent dielectric studies. These studies reveal that the NaAlO₂ fillers participate actively in the ion transport and enhance free Na⁺ ions in the electrolyte system. However, at higher concentration, these particles start blocking the ion transport and may form an ion multiplate and hence reduce the ionic conductivity.
- (5) The electrochemical stability window and the cation (Na⁺) transport number of the electrolyte system improved significantly on dispersion of these active fillers. The optimized electrolyte composition carrying 5 wt.% NaAlO₂ possessed a stability window of ~ 4.5 V and cation transport number of ~ 0.60.

Acknowledgments We wish to thank Jaypee Institute of Information Technology (JIIT), Noida, for providing the XRD facility (XRD-6000, SHIMADZU).

Funding We acknowledge the financial support received from Science and Engineering Research Board, a statutory body of the Department of Science and Technology, Government of India (File No: YSS/2015/001234).

Data Availability The raw/processed data required to reproduce these findings cannot be shared at this time, as the data also forms part of an ongoing study.

Declarations

Conflict of interest The authors declare that they have no known competing financial interests or personal relationships that could have appeared to influence the work reported in this paper.

Consent to participate All the authors agree to participate in this research communication

Consent for publication The authors have consented to the submission of the manuscript to the journal.

References

1. H. Li, X. Zhang, Z. Zhao, Z. Hu, X. Liu, and G. Yu, *Energy Storage Mater.* 26, 83 (2020).
2. Y. Liu, Z. Sun, K. Tan, D.K. Denis, J. Sun, L. Liang, L. Hou, and C. Yuan, *J. Mater. Chem. A* 7, 4353 (2019).
3. K. Mishra, N. Yadav, and S.A. Hashmi, *J. Mater. Chem. A* 8, 22507 (2020).
4. M.S. Syali, D. Kumar, K. Mishra, and D.K. Kanchan, *Energy Storage Mater.* 31, 352 (2020).
5. F. Gebert, J. Knott, R. Gorkin, S.L. Chou, and S.X. Dou, *Energy Storage Mater.* 36, 10 (2021).
6. K.S. Ngai, S. Ramesh, K. Ramesh, and J.C. Juan, *Ionics* 22, 1259 (2016).
7. L. Fan, C.W. Nan, and S. Zhao, *Solid State Ion.* 164, 81 (2003).
8. J. Cui, Z. Zhou, M. Jia, X. Chen, C. Shi, N. Zhao, and X. Guo, *Polymers* 12, 1324 (2020).
9. B. Liang, S. Tang, Q. Jiang, C. Chen, X. Chen, S. Li, and X. Yan, *Electrochim. Acta* 169, 334 (2015).
10. Y.L. Ni'mah, M.Y. Cheng, J.H. Cheng, J. Rick, and B.J. Hwang, *J. Power Sources* 278, 375 (2015).
11. S.N. Banitaba, D. Semnani, B. Rezaei, and A.A. Ensafi, *Polym. Adv. Technol.* 30, 1234 (2019).
12. M.C. Dimri, D. Kumar, S.B. Aziz, and K. Mishra, *Ionics* 27, 1143 (2021).
13. F. Croce, L. Persi, B. Scrosati, F. Serraino-Fiory, E. Plichta, and M.A. Hendrickson, *Electrochim. Acta* 46, 2457 (2001).
14. C. Ma, K. Dai, H. Hou, X. Ji, L. Chen, D.G. Ivey, and W. Wei, *Adv. Sci.* 5, 1700996 (2018).
15. I. Nicotera, C. Simari, M. Agostini, A. Enotiadis, and S. Brutti, *J. Phys. Chem. C* 123, 27406 (2019).
16. Z. Zhang, K. Xu, X. Rong, Y.S. Hu, H. Li, X. Huang, and L. Chen, *J. Power Sources* 372, 270 (2017).
17. Y. Wang, Z. Wang, J. Sun, F. Zheng, M. Kotobuki, T. Wu, K. Zeng, and L. Lu, *J. Power Sources* 454, 227949 (2020).
18. S.A. Hashmi, M.Y. Bhat, M.K. Singh, N.T. Kalyana Sundaram, B.P.C. Raghupathy, and H. Tanaka, *J. Solid State Electrochem.* 20, 2817 (2016).
19. A.K. Chauhan, D. Kumar, K. Mishra, and A. Singh, *Mater. Today Comm.* 26, 101713 (2021).
20. P.G. Bruce, and C.A. Vincent, *J. Electroanal. Chem.* 225, 1 (1987).
21. P.G. Bruce, J. Evans, and C.A. Vincent, *Solid State Ion.* 28–30, 918 (1988).
22. M. Marzantowicz, J.R. Dygas, F. Krok, J.L. Nowinski, A. Tomaszewska, Z. Florjanczyk, and E.Z. Monikowska, *J. Power Sources* 159, 420 (2006).
23. M.S. Lisowski, Q. Liu, J. Cho, J. Runt, F. Yeh, and B.S. Hsiao, *Macromolecules* 33, 4842 (2000).
24. C.S. Liao, and W.B. Ye, *Electrochim. Acta* 49, 4993 (2004).
25. Z. Liu, X. Wang, J. Chen, Y. Tang, Z. Mao, D. Wang, and A.C.S. Appl, *Energy Mater.* 4, 623 (2021).
26. S.B. Aziz, T.J. Woo, M.F.Z. Kadir, and H.M. Ahmed, *J. Sci. Adv. Mater. Dev.* 3, 1 (2018).
27. S. Patra, P. Thakur, B. Soman, A.B. Puthirath, P.M. Ajayan, S. Mogurampelly, V.K. Chethan, and T.N. Narayanan, *RSC Adv.* 9, 38646 (2019).

28. M.A. Brza, S.B. Aziz, M.M. Nofal, S.R. Saeed, S. Al-Zangana, W.O. Karim, S.A. Hussien, R.T. Abdulwahid, and M.F.Z. Kadir, *Polymers* 12, 1885 (2020).
29. A. Kumar, M. Madaan, A. Arya, S. Tanwar, and A.L. Sharma, *J. Mater. Sci. Mater. Electron.* 31, 10873 (2020).
30. P. Singh, P.N. Gupta, and A.L. Saroj, *Phys. B Condens. Matter* 578, 411850 (2020).
31. A.K. Jonscher, *Nature* 167, 673 (1977).
32. R. Kumar, and S.A. Suthanthiraraj, *J. Non-Cyst. Solids* 405, 76 (2014).
33. N. Srivastava, and M. Kumar, *Solid State Electrochem.* 20, 1421 (2016).
34. K. Funke, *Prog. Solid State Chem.* 22, 111 (1993).
35. Y.Y. Wang, A.L. Agapov, F. Fan, K. Hong, X. Yu, J. Mays, and A.P. Sokolov, *Phys. Rev. Lett.* 108, 088303 (2012).
36. M. Kumar, T. Tiwari, A.K. Chauhan, and N. Srivastava, *Mater. Res. Express* 1, 045003 (2014).

Publisher's Note Springer Nature remains neutral with regard to jurisdictional claims in published maps and institutional affiliations.